Historical changes in 239Pu and 240Pu sources in sedimentary records in the East China Sea: Implications for provenance and transportation

Wang, Jinlong; Baskaran, Mark; Hou, Xiaolin; Du, Jinzhou; Zhang, Jing

Published in:
Earth and Planetary Science Letters

Link to article, DOI:
10.1016/j.epsl.2017.03.005

Publication date:
2017

Document Version
Peer reviewed version

Historical Changes in ^{239}Pu and ^{240}Pu Sources in Sedimentary Records in the East China Sea: Implications for provenance and transportation

Jinlong Wang[1], Mark Baskaran[2], Xiaolin Hou[3,4],Jinzhou Du[1,*], and Jing Zhang[1]

[1]State Key Laboratory of Estuarine and Coastal Research, East China Normal University, Shanghai 200062, P. R. China

[2]Department of Geology, Wayne State University, Detroit, Michigan, 48202-3622, USA

[3]Center for Nuclear Technologies, Technical University of Denmark, Risø Campus, Roskilde 4000, Denmark

[4]Xi'an AMS Center, SKLLQG, Institute of Earth Environment, CAS, 710061, Xi'an, P. R. China

(*Corresponding author. Tel.:+86-21-62232761; Fax: +86-21-62546441. E-mail address: jzdu@sklec.ecnu.edu.cn)

Highlights:

- The Yangtze River Pu input is the dominant source of Pu near the Yangtze Estuary
- The PPG input dominated the Pu mass balance in the East China Sea
- Pu is a better chronology time marker compared to ^{137}Cs in the marine environment and ^{137}Cs cannot be used as a reliable chronometer in marine environment.

Abstract:

Concentrations and isotopic composition of plutonium (Pu) are widely used for its source identification and to determine transport processes of Pu-associated particulate matter and water. We investigated the concentrations of ^{239}Pu and ^{240}Pu and their ratios in a number of sediment samples from the East China Sea (ECS) collected in summer (August 6-28) in 2013. The $^{239+240}$Pu activity concentrations in surface sediment samples were found to range between 0.048 and 0.492 Bq kg^{-1} and the ^{240}Pu/^{239}Pu atom ratios showed a similar trend as that of the $^{239, 240}$Pu activities; the Pu atom ratios ranged from 0.158 to 0.297, and were mostly higher than the mean global fallout value of 0.18. The $^{239, 240}$Pu inventories in the ECS varied widely, from 2 to 807 Bq m^{-2}, and highest values commonly found in the coastal areas. In the Yangtze Estuary, the mean $^{239+240}$Pu activity concentration is close to the estimated erosional input value of 0.18 Bq kg^{-1}, and the ^{240}Pu/^{239}Pu atom ratio was found to be ~ 0.18, which indicates that the riverine input is the dominant source of Pu for this area. However, the total annual Yangtze River input of $^{239+240}$Pu was estimated to be 2.4 $\times10^{10}$ Bq, which is small compared to the total amount of buried $^{239+240}$Pu, 3.1×10^{13} Bq in the whole ECS. The Pacific Proving Ground input appears to be the dominant source of Pu to the ECS, accounting for 45%-52% of the total inventory. The fractional amount of Pu scavenged by the Kuroshio Current (KC) and Taiwan Warm Current (TWC) into ECS sediments is estimated to be ~10%. A small fraction of Pu in the ECS could have originated from the Yellow Sea, transported by coastal currents. ^{240}Pu/^{239}Pu atom ratio is useful not only to obtain a better insight of the biogeochemistry influenced by the KC, but also to trace the long-range transport of other particle-reactive radionuclides. Besides, the sedimentation rates obtained based on excess ^{210}Pb and the penetration depths of $^{239+240}$Pu agreed quite well. Compared to ^{137}Cs, the $^{239+240}$Pu can be used as a better chronostratigraphic time marker in marine environment.

Key words: East China Sea; plutonium; isotopic ratio; sediment; transportation; mass balance;

1. Introduction

^{239}Pu (half-life of 2.41 × 10^4 yr) and ^{240}Pu (half-life of 6.56 × 10^3 yr) in the environment are derived from thermonuclear bomb testing (e.g., MIKE in 1952 and BRAVO in 1954), which resulted in a large amount of global fallout (e.g. Donaldson et al., 1997), nuclear accidents (e.g., Chernobyl and Fukushima) (Clark and Smith, 1988; Zheng et al., 2012) and nuclear reprocessing facilities and nuclear power plants (Peirson et al., 1982). Among the transuranic elements, concentrations of plutonium isotopes (^{239}Pu, ^{240}Pu) and their ratios have been most widely used tracers and chronometers in aqueous and terrestrial environments. Vertical profiles of Pu isotopes in coastal and lacustrine sediments provide chronology for the past 60-65 years which is useful for the reconstruction of the temporal nutrient supply variations, organic and inorganic pollution history and biological productivity (Santschi et al., 1980; Ravichandran et al., 1995; Baskaran et al., 1996). Pu, with higher particle reactivity, could also be used to validate excess ^{210}Pb-based chronology in coastal areas. A comparison of the direct atmospheric fallout record of Pu (as determined from the atmospheric fallout record of ^{90}Sr) with that preserved in sediment cores is useful to infer the effects of sediment resuspension and/or mixing due to physical and/or biological processes. Moreover, the vertical distribution of Pu in sediment cores in conjunction with excess ^{210}Pb is used to delineate sediment mixing rate from sediment accumulation rates (e.g., Buffoni et al., 1992; Ravichandran et al., 1995; Su and Huh, 2002).

The ^{240}Pu/^{239}Pu ratios in the marginal seas of the Pacific Ocean vary depending on the sources of plutonium; an average ^{240}Pu/^{239}Pu atom ratio of global fallout is 0.176 ± 0.014 (Krey, 1976; Kelley et al., 1999), which is distinctly different from ratios of 0.33 - 0.36 in the Pacific Proving Grounds (PPG) in the Marshall Islands (mainly Bikini and Enewetak Atolls) (Buesseler, 1997). In the North Pacific Ocean, the principal source of Pu is close-in (tropospheric) fallout from nuclear weapons testing at the PPG and global (stratospheric) fallout, and the local regional fallout of ^{239}Pu and ^{240}Pu was estimated to be 2.4 PBq and 2.7 PBq (Hamilton, 2004), respectively. Pu from the Marshall Islands have been reported to have spread widely into the North Pacific Ocean, especially the Northwest Pacific, due to the westward flowing North Equatorial Current (NEC) (Povinec et al., 2003). The velocity of surface water-associated radionuclides transported by the NEC is approximately 13-18 km day^{-1} (Donaldson et al., 1997). Therefore, Pu from the PPG can be transported to long distances into the adjacent marginal seas of the western Pacific Ocean in less than one

year and can subsequently reach the East China Sea (ECS) via the Kuroshio Current (Wang and Yamada, 2005; Liu et al., 2011). Thus the characteristic $^{240}Pu/^{239}Pu$ atom ratio makes it an important tool to track the sources of Pu in the East China Sea.

ECS is one of the world's typical river-dominated ocean margin systems with a large river input and complex current system. The Yangtze River is the largest river on the Eurasian continent, discharging a large amount of water and sediment into ECS, although sediment discharge has been reduced by 75% since 2000, due to the construction of impoundments (Dai et al., 2013; 2014). 40-50% of the river-derived sedimentary particles deposited near the estuary aa fraction of which is subsequently transported offshore, mostly southward along the coasts of Zhejiang and Fujian Provinces (McKee, et al., 1983). The large riverine sediment discharge and complex current system result in ECS having high concentration of suspended particles, which makes East China Sea potentially act as one of most important "sinks" for Pu originated in the PPG, compared to other adjacent marginal seas of the western Pacific Ocean. On a broader context, this is relevant to other long-range transport of other particle-reactive radionuclides such as ^{210}Pb, ^{230}Th, ^{231}Pa, etc. Moreover, there are limited studies on the use of Pu as a chronological tool in the ECS (Huh and Su, 1999).

In recent years, several investigations have been carried out to determine $^{239+240}Pu$ in the ECS (Nagaya and Nakamura, 1992; Su and Huh, 1999; 2002; Wang and Yamada, 2005; Liu et al., 2011). However, ^{239}Pu and ^{240}Pu data in the Yangtze River catchment are very limited, which limits an accurate estimation of the contribution from the Yangtze River input, and determination of a reliable Pu mass balance for the ECS. The objective of this work is to determine the concentrations and isotopic ratios of ^{239}Pu and ^{240}Pu in surface sediments and sediment cores in the ECS and to investigate the sources and mass balance of Pu evaluated from the inventories of ^{239}Pu and ^{240}Pu and their atomic ratios. Besides, the sedimentation rate estimation is conducted to compare the Pu, ^{137}Cs and $^{210}Pb_{ex}$ based chronology methods in marine environment. It is expected that this studywill provide insights on the processes and mechanisms that control the transport and fate of Pu and other species that behave similar to Pu, using a simple mass balance of Pu for the ECS.

2. Materials and Methods:

2.1 Study area

The ECS is a marginal sea and has a very wide and flat continental shelf, with a total area of 7.7×10^5 km^2, a maximum width of 640 km, and a mean water depth of

72 m. The major current system in the ECS is very complicated, as was described in Su (2001) (Fig. 1). The freshwater from the Yangtze River flows into the estuary and subsequently flows towards the south in winter and turns to the northeast in summer. In the southern part, there are two northward currents of which one is the warm and salty Kuroshio Current (KC) along the continental shelf break of the ECS, with a branch turning into the Yellow Sea known as the Yellow Sea Warm Current (YSWC), and the other is the Taiwan Warm Current (TWC) moving northward from the Taiwan strait. Along the coast, the southeastern North Jiangsu Coastal Current （NJCC）flows to the north of the Yangtze River mouth and the southwestern Zhejiang-Fujian Coastal Current（ZFCC）flows to the south of the Yangtze River mouth. In summer, the northward TWC intensifies and the southward ZFCC weakens under the prevailing southeast monsoon. The Yellow Sea Coastal Current (YSCC) is parallel to the NJCC in the middle of the Yellow Sea and intersects with the YSWC and the TWC to form a counterclockwise circulation.

2.2. Sampling and analysis

Sediment samples, including 23 surface sediments (0-2 cm) and 6 sediment cores (Fig. 1b), were collected during the R/V “Dongfanghong 2” Cruise in August of 2013 using a box corer. The sediment cores were collected with 10-cm diameter Plexiglas core tubes and were sliced in 1-cm interval using a stainless steel knife and were stored in resealable plastic bags at 4 °C until laboratory analysis. Visual observations of the cores were also recorded.

An aliquot of 2 g of dry sediment equivalent was used for the measurement of grain size using a laser particle analyzer (LS100Q, Beckman, USA). 60-120 g dried sample was homogeneously pulverized and sealed in a plastic container (70 mm diameter × 70 mm height) for at least three weeks to establish a secular equilibrium between ^{226}Ra and daughter products of ^{222}Rn before measurement. The activity concentrations of $^{210}Pb_{ex}$ in sediment samples were measured following the method described by Du et al. (2010). The activities of ^{137}Cs, ^{226}Ra and ^{210}Pb were measured using HPGe γ-ray spectrometry (Canberra Be3830) with 35% relative counting efficiency and had an energy resolution of 1.8 keV (at 1332 keV) (Du et al., 2010). The activity of $^{210}Pb_{ex}$ was calculated from the measured total ^{210}Pb (46.5 keV, branching ratio: 4.25%) minus the parent-supported ^{210}Pb activity which is assumed to be the same as the ^{226}Ra activity. ^{226}Ra was determined using the gamma line at 351.9 keV (37.6%) for ^{214}Pb and 609.3 keV (46.1%) for ^{214}Bi. The activity of ^{137}Cs was determined from the gamma ray peak at 661.6 keV (85%). The efficiency calibration

of the detector system was conducted using both the Laboratory Sourceless Calibration Software (LabSOCS) and sediment standard (GBW04127= was diluted by homogeneously mixed with natural marine sediment (< 63 μm); the activities of the radionuclides were certified by producer (e.g., Dai et al., 2011; Wang et al., 2016a).

The separation method of Pu was modified from Xu et al. (2014). Briefly, 5-20 g dried sediment samples were first ashed at 550 °C overnight. After spiking with 6-10 mBq ^{242}Pu (NIST-SRM-4334G), the residue was leached with 50-200 mL aqua regia at 200 °C for 2 h. After filtration through a GF/A filter, plutonium in the leachate was coprecipitated with iron hydroxides by adding NH_3OH. The precipitate was separated by centrifugation. The precipitate was washed with 2 mol L^{-1} NaOH and then was dissolved with ~3 mL of concentrated HCl. To this solution, ~650 mg of $K_2S_2O_5$ was added to reduce the overall Pu to Pu(III). The pH of the solution was adjusted to ~9-10 by adding ammonium. The precipitate was separated by centrifugation and then dissolved with ~4 mL of concentrated HCl and 3 mL of concentrated HNO_3 for the oxidation of Pu(III)–Pu(IV) by NO_2^- in the HNO_3 solution. The solution was gently evaporated to near dryness and 5 mL of 8 mol L^{-1} HNO_3 was added to dissolve the residue. The solution was loaded on to a preconditioned AG 1-×4 anion-exchange column (1.0 cm in diameter and 20-cm height, 50-100 mesh, Cl- form). After rinsing the column with 8 mol L^{-1} HNO_3 and 9 mol L^{-1} HCl to remove most uranium, thorium and other matrix elements, Pu was eluted with 70 mL of 0.5 mol L^{-1} HCl. Pu in the eluate was co-precipitated with $Fe(OH)_3$ after adding 100 mg of Fe^{3+} ($FeCl_3$), then the redox pair of $K_2S_2O_5$-conc. HNO_3 was used to adjust overall Pu to Pu(IV). The final sample solution prepared in 1 mol L^{-1} HNO_3 was loaded to a TEVA column (2 mL, 200 mesh). After rinsing with 60 mL of 1 mol L^{-1} HNO_3 and 60 mL of 6 mol L^{-1} HCl, Pu was finally eluted with 40 mL of 0.1 mol L^{-1} $NH_2OH{\cdot}HCl$ in 2 mol L^{-1} HCl. The elute was evaporated to dryness on a hot-plate followed by adding 7-10 mL of concentrated nitric acid and heating at 200 °C to decompose the hydroxylamine hydrochloride. The residue was finally dissolved in 0.5 mol L^{-1} HNO_3 and In (III) (as $InCl_3$) was added as an internal standard for measurement of ^{239}Pu and ^{240}Pu by the ICP-MS (X Series II, Thermo Fisher Scientific, Waltham, MA) equipped with an Xs-skimmer cone and an ultrasonic nebulizer (U5000AT+, CETAC, USA) under hot plasma conditions. The chemical yield was found to range between 64% and 96% (mean: 72%±16%). Determination of ^{239}Pu and ^{240}Pu in separated samples was conducted using an inductively coupled plasma mass spectrometer (ICP-MS) The separation of Pu using anion exchange chromatography followed by extraction

chromatography (TEVA column) ensures sufficient removal of uranium, which interferes the measurement of ^{239}Pu by tailing and $^{1}H^{238}U$ ion. Uranium remained in the separated sample was monitored by measurement of ^{238}U to be less than 0.02ppb (for detailed information, Qiao et al., 2014 and Xu et al., 2014). A certified reference material (IAEA-376, marine sediment) was analyzed with the samples, and the analytical results of ^{239}Pu and ^{240}Pu agree well with the certified values.

3. Results and discussions

3.1. The spatial distribution of Pu isotopes in surface sediments of the ECS

The activity concentrations of Pu isotopes and $^{210}Pb_{ex}$ along with grain size are given in the supplementary material. The $^{239+240}$Pu activity concentrations in surficial sediments (Fig. 2c) ranged between 0.048±0.004 and 0.492±0.035 Bq kg^{-1} (mean: 0.188±0.119 Bq kg^{-1}). The activity concentration of ^{239}Pu and ^{240}Pu varied between 0.026±0.003 and 0.246±0.025 Bq kg^{-1} (mean: 0.099 ± 0.057) and 0.022±0.002 and 0.247±0.025 Bq kg^{-1} (mean: 0.088 ± 0.061 Bq kg^{-1}), respectively (Fig. 2a, b). The spatial distribution of radionuclides activities (Fig. 2) were produced by the Surfer mapping software package using Kriging interpolation based on a digital elevation model (DEM) with 6 × 6 km grid resolution. The lowest Pu concentrations were observed near the Yangtze Estuary and Hangzhou Bay, with a range of 0.048±0.004 to 0.186±0.014 Bq kg^{-1}. The sedimentation rate in these regions showed higher values of > 2 cm y^{-1} (Huh and Su, 1999), so the low $^{239+240}$Pu activity is likely related to dilution of massive influx of river-borne sediments. The Pu concentrations in sediments north of the ECS region were also low. A decreasing trend of $^{239+240}$Pu concentrations in sediments from the offshore towards the northwest was also observed, which is similar to the direction of the YSWC. In contrast, the maximum $^{239+240}$Pu concentration was observed on the transportation pathway of the TWC and decreased towards inshore, suggesting that the TWC likely plays an important role in the transport of Pu from the open sea. The measured ^{239}Pu and ^{240}Pu concentrations in surface sediment in this work are comparable to the reported values in the ECS and other marginal seas of the Pacific Ocean such as the Yellow Sea (0.13 - 0.35 Bq kg^{-1}, mean: 0.23 Bq kg^{-1}) (Nagaya and Nakamura, 1992) and the South China Sea (0.16 - 0.79 Bq kg^{-1}, mean: 0.50 Bq kg^{-1}) (Wu et al., 2014) but are much lower than the values observed in the Okinawa Trough (1.4 - 2.5 Bq kg^{-1}, mean: 1.8 Bq kg^{-1}) (Wang and Yamada, 2005) and the northwest Pacific Ocean (0.15 - 5.4 Bq kg^{-1}, mean: 2.4 Bq kg^{-1}) (Moon et al., 2003). This variation in different areas may indicate a pathway of Pu from the PPG transported by the NEC and the KC.

3.2 Distribution of $^{240}Pu/^{239}Pu$ atom ratios and sources term of Pu in the ECS

The $^{240}Pu/^{239}Pu$ atom ratios in sediment cores from the ECS (Fig. 2d) ranged from 0.158±0.022 to 0.297±0.042 (mean: 0.238±0.036), which was between global fallout value of 0.18 ± 0.02 (Krey et al., 1976) and PPG close-in fallout value of 0.33-0.36 (Buesseler, 1997). The major inputs of Pu to this area is likely derived from: 1) atmospheric fallout from weapons testing, 2) the close-in fallout (tropospheric) in PPG, 3) riverine input from the erosion and leaching of soils in the watershed of Yangtze River, 4) emission from the nuclear reprocessing plants, 5) nuclear accidents (e.g. Chernobyl and Fukushima accidents) and 6) transport of effluents from adjacent sea area (e.g., Yellow Sea).

3.2.1 The close-in fallout and emission from the nuclear power plants

From Figure 3, the distribution of $^{240}Pu/^{239}Pu$ atom ratios were ~0.18 in Chinese (Zheng et al., 2009; Dong et al., 2010; Liu et al., 2013； Bu et al., 2014) and Japanese soils profiles (Muramatsu et al., 1999, 2003), which implies that the direct input from the close-in fallout from Semipalatinsk, Lop Nur nuclear tests and Chernobyl and Fukushima accidents did not give a significant contribution to the source of Pu in these areas, due to their distinctive $^{240}Pu/^{239}Pu$ atom ratios of 0.03-0.05 (Beasley et al., 1998) , < 0.1 (Wu et al., 2010), 0.31-0.40 (Boulyga et al., 1997) and 0.32-0.33 (Zheng et al., 2012), respectively. Considering the location of the ECS is far away from the any sites of nuclear weapons testing, and the catchment of the rivers flowing into the ECS is also far from the Chinese weapons testing site, Pu contribution from the close-in fallout of the Chinese weapons testing appears to be negligible here. There were 14 nuclear power reactors (as of August 2013) operating along the Chinese coast in the ECS. However, all Pu was produced and confined in the fuel elements, and there is no report on the leakage of nuclear fuel from **a**ny of these NPPs, the contribution from the Chinese NPPs would be negligible.

3.2.2 Riverine input from the erosion and leaching of soils

The Yangtze River and the Yellow River load huge amounts of sediments to China's marginal seas and are the potential riverine source of $^{239,240}Pu$ to the ECS. It has been reported that the $^{240}Pu/^{239}Pu$ atom ratios in both of these river catchments are 0.18 (Zheng et al., 2009; Dong et al., 2010; Bu et al., 2014) and that the riverine Pu eventually originates from the global atmospheric fallout. Moreover, there are several small rivers that flow into the ECS from the Zhe-Min coast but the contributions from these rivers are likely negligible considering the relatively small amount of water and sediment discharge (e.g., the largest catchment of all smaller

rivers, streams and tributaries is Min River catchment with an area of 61,000 km^2, CWRC, 2013). Because of very limited published Pu data in the Yangtze watershed, the reported river-borne input of $^{239+240}Pu$ has high uncertainty. Recently, some investigations of Pu isotopes in soils and sediments of the Yangtze river catchment (Liao et al, Dong et al., 2010; Bu et al., 2014) have been conducted, which enables us to obtain a better estimation of the river input of Pu. Smith et al. (1987) and Dominik et al. (1987) investigated several catchments and estimated the residence time of Pu from soil to be 800-3,000 yr. The Yangtze catchment is one of the largest river catchments in the world and contains many dams (e.g., The Three Gorges Dam); therefore, we used the largest value of the range (3,000 yr) as the watershed residence time of Pu. It can be calculated that 0.023% of the Pu in the drainage catchment is eroded each year. The Yangtze River input of $^{239+240}Pu$ was calculated following the equation (modified from previous studies: Ravichandran et al., 1995; Baskaran et al., 1997):

$$I_{Pu} = A_d * I_f * f_e \quad (1)$$

where A_d is the area of the catchment (1.8×10^{12} m^2), I_f is the inventory of $^{239+240}Pu$ (Bq m^{-2}) and f_e is the fraction of the inventory of $^{239+240}Pu$ eroded each year (0.023%). The inventories of $^{239+240}Pu$ in soils of the Yangtze catchment listed in Table 2 range from 19.0 ± 1.6 to 114 ± 5.9 Bq m^{-2} (arithmetic mean: 59 ± 35 Bq m^{-2}). The mean Pu input derived from the Yangtze River was calculated to be $(0.79\pm0.07)\times10^{10}$-$(4.7\pm0.2)\times10^{10}$ Bq y^{-1} (arithmetic mean: $(2.4 \pm 1.4) \times10^{10}$ Bq y^{-1}). The Yangtze River delivers approximately 1.3×10^8 tons yr^{-1} of terrestrial sediment to the ECS (CWRC, 2013). Therefore, the mean $^{239+240}Pu$ activity concentration in the suspended materials eroded from the drainage area was calculated to be 0.06±0.01 - 0.36 ± 0.02 Bq kg^{-1} (mean: 0.18 ± 0.10 Bq kg^{-1}), which was close to the values of surface sediments near the Yangtze Estuary and Hangzhou Bay (Fig. 3). Considering the $^{240}Pu/^{239}Pu$ atom ratios are ~0.18 in this area, we suggest that the Yangtze River input is the main source of Pu isotopes for the estuarine area in the ECS. Liu et al. (2011) also suggested that the dilution of riverine input played an important role in the distribution of Pu isotopes near the Yangtze Estuary (Liu et al., 2011). The magnetic minerals and particulate heavy metals in this area have also been reported to be from the Yangtze River input (Che et al., 2003; Liu et al., 2010). This is because ~ 50% of the Yangtze River-derived fine sediments were deposited near the Yangtze Estuary and Hangzhou Bay under the cumulative action of delivery by the CDW and the barrier effect from the northward flowing TWC (Che et al., 2003; Liu et al., 2006).

All these observations support that soil erosion in the Yangtze River catchment contributes the major fraction of Pu to the estuarine sediment.

3.2.3 Long-range transport from the PPG

Fukushima accident has been reported to release a very small amount of Pu to marine environment (Zheng et al., 2012), thus the long distance transport from Fukushima coastal waters to the ECS is negligible. However, the Pu derived from the PPG transport has been suggested to be an important source of $^{239+240}$Pu (Lee et al., 2004; Zheng and Yamada, 2004; Wang and Yamada, 2005; Liu et al., 2011). The distribution of ^{240}Pu/ ^{239}Pu atom ratios in surficial sediments (including sediment cores) and seawater (Fig. 3) around the NEC and KC pathway showed a similar variation pattern with a mean atom ratio of ~0.24 (e.g., Kim et al., 2004; Zheng and Yamada, 2004; Yamada et al., 2006). A strong signature of the PPG Pu was recorded in a natural coral of Guam site with a mean atom ratio of 0.31 (Lindahl et al., 2011). The spatial distribution of the ^{240}Pu/^{239}Pu atom ratio coincided with the water mass distribution in the ECS, which apparently shows the influence of transport of Pu from PPG inputs by the Kuroshio Current and the TWC. These observations further support that Pu could transport from the PPG into the ECS. As a particle-reactive nuclide in marine environment, the dissolved Pu in ECS can be removed from the water column into sediments by particle scavenging, after the advective lateral transport from the open ocean to the ocean margin (Zheng and Yamada, 2006).

The riverine input and global fallout $^{239+240}$Pu can be regarded as one end-member considering their same ^{240}Pu/^{239}Pu atomic ratios. A simple two end-member mixing model described by Krey et al. (1976) was used to estimate the relative contribution of plutonium isotopes from global fallout and PPG in the ECS:

$$\frac{(Pu)_P}{(Pu)_G} = \frac{(R_G - R_E)(1+3.68R_P)}{(R_E - R_P)(1+3.68R_G)} \quad (2)$$

where (Pu) and R represent the $^{239+240}$Pu activity concentration and the ^{240}Pu/^{239}Pu atom ratio, respectively. The subscripts P, G and E refer to the PPG, global fallout, and the ECS, respectively. The constant 3.68 is the ratio of the decay constant of ^{240}Pu/^{239}Pu which is used to convert the activity ratio to the atomic ratio. The R_G and R_P are 0.18 and 0.33-0.36, respectively (Krey et al. 1976; Buesseler, 1997). The calculated results showed that the contributions of Pu from the PPG to surface sediment of the ECS ranged from < 1% to 72% ± 7%, with mean value of 41% ± 6% (R_P = 0.36), and from < 1% to 82% ± 8%, with mean value of 47% ± 7% (R_P = 0.33). Apparently, the PPG input had a great influence on the sedimentary Pu in the ECS

and is found to be the main source of Pu to the ECS.

3.3. Temporal Variations of Pu in the sediment cores in the ECS

3.3.1 Sedimentation rates

The detailed information of vertical profiles of Pu isotopes are listed in supplemental file (Table A. 2). Assuming that the sedimentation rates did not change drastically over the past 61 years, the linear sedimentation rates obtained from the vertical profiles of $^{210}Pb_{ex}$ in the ECS were: 0.83±0.48, 0.77±0.10, 0.32±0.03, 0.38±0.07, 0.13±0.01 and 0.13±0.02 cm y^{-1} at C1, E1, M7, B6, C12 and F8 sites, respectively (Fig. 4). The depth corresponding to maximum $^{239+240}Pu$ activity concentration varied in these cores due to variable sedimentation rates. The relatively low resolution of Pu in sediment cores prevented us from identifying the exact depth layer where the $^{239+240}Pu$ concentration peak corresponding to 1963 which would have resulted in getting better mean sedimentation rate. The penetration depths of Pu corresponding to 1952, when many high yield nuclear weapons tests were started (i.e. PPG), can be used as a chronological marker to determine independent sedimentation rate. The lowest $^{239+240}Pu$ concentrations measured in the bottom layers of cores E1, M7, B7, C12 and F8 (Fig. 5) are near the detection limits of $^{239+240}Pu$ (0.01 Bq kg^{-1}). These bottom layers could be seen as the penetration depths of Pu corresponding to 1952. Considering the uncertainty (1.5 cm) from sedimentary particle compaction during sub-sectioning,the estimated mean sedimentation rates were estimated to be 0.78±0.02, 0.38±0.02, 0.35±0.02, 0.20±0.02 and 0.14±0.02 cm y^{-1} at E1, M7, B6, C12 and F8, respectively. The discernible concentration peak for ^{137}Cs corresponding to 1963 was not observed in six cores (Fig. 4). This observation is due to the higher mobility of ^{137}Cs due to low K_d (< 500) in marine systems (Cochran et al., 1995; Delfanti et al., 2003; Wang et al., 2016). We attempted to use the penetration depths of ^{137}Cs in C12 (4.5-6.5 cm) and F8 (4.5-6.5 cm) to roughly estimate the sedimentation rates to be 0.09±0.05 cm y^{-1} at these two cores, but these rates are not reliable.

C1 is located near the river mouth, where there is reworked mobile mud and sediment commonly undergoes erosion (Yang et al., 2011; Wang et al., 2016). Thus, the estimated sedimentation rate of the C1 core by $^{210}Pb_{ex}$ is less reliable and significantly lower than the reported value of 3.0 cm y^{-1} (Su and Huh, 2002). Considering the high sedimentation rate and short length of core C1 (42 cm), it is not able to evaluate the sedimentation rate of C1 by $^{239+240}Pu$ or ^{137}Cs. The sedimentation rates estimated in this work using Pu isotopes are comparable to the data published in literature (0.5 - 0.8 cm y^{-1} for E1, 0.3 - 0.5 cm y^{-1} for M7 and B6, 0.1 - 0.2 cm y^{-1} for

C12 and F8, Su and Huh, 2002). The sedimentation rates estimated by ^{137}Cs were much lower than those based on $^{239+240}Pu$ and $^{210}Pb_{ex}$ in core C12 and F8. This is likely related to the longer residence time of ^{137}Cs in ocean water and ^{137}Cs does not trace sedimentary particles (Lee et al., 2004). However, the sedimentation rates estimated by $^{239+240}Pu$ agree well with those by $^{210}Pb_{ex}$ in the other 5 cores (R^2=0.97, $p<0.01$). Compared to ^{137}Cs, $^{239+240}Pu$ is a better time marker to validate the $^{210}Pb_{ex}$ chronology in marine environment and ^{137}Cs is not suitable chronometer in marine environment.

3.3.2 The vertical variations of Pu isotope composition in the sediment cores

The vertical distribution of $^{240}Pu/^{239}Pu$ atom ratios in the sediment cores (Fig. 5 and Table A. 5) shows that the Pu derived from PPG is the major source of Pu in the ECS (except C1), with a PPG contribution portion of > 50% in most layers (R_p = 0.33).. The atomic ratio of $^{240}Pu/^{239}Pu$ in deep layers of cores E1, B6 and F8 varied between 0.269 and 0.314, which are close to those observed in the close-in fallout at the PPG. The trend of mean $^{240}Pu/^{239}Pu$ atomic ratios in the sediment cores in the ECS (E1 > C1, F8 > B6 > M7; Table 2) are consistent with the flow direction of the TWC and the KC in the ECS. Both F8 and C12 are located in the pathway of the KC and continental shelf margin, but $^{240}Pu/^{239}Pu$ atom ratios in C12 were relatively lower than that in F8. A previous study also reported a lower value in the upper layer of a sediment core in the same area (SST1, 0.21-0.26, Wang and Yamada, 2005), which may be attributed to other input source of Pu with lower $^{240}Pu/^{239}Pu$ atom ratio (e.g., terrestrial input) for C12. C12 is located in the north Okinawa Trough, which is one of important sinks of fine sedimentary particles in the ECS. Previous studies have suggested that these fine particles in the north Okinawa trough were mostly derived from terrestrial particles input, including Yangtze input and finer particles from Taiwan (e.g., Oguri et al., 2003; Dou et al., 2010; Li et al., 2015). As has been discussed above, these terrestrial particles had a lower $^{240}Pu/^{239}Pu$ atom ratio of 0.18. Therefore, the lower $^{240}Pu/^{239}Pu$ atom ratio was observed in the north Okinawa trough.

3.4. Inventory of Pu in the ECS sediment cores

The inventories of Pu (= ^{239}Pu inventory + ^{240}Pu inventory) and $^{210}Pb_{ex}$ were obtained from the activity in the measured layers and the interpolated activity for those layers where the radionuclides were not measured (inventory for a layer = activity in that layer (or interpolated activity for that layer) × mass depth of that layer). The calculated inventories for total Pu and the excess ^{210}Pb are: 35.6±2.5, 118±5.0, 65.4±2.5, 58.3±4.6, 33.9±0.7, 1.9±0.1 Bq m^{-2} and 12.3±1.5, 14.9±2.1, 6.7±5.4,

13.1±1.2, 29.2±1.6, 3.2±0.9 kBq m^{-2} at C1, E1, M7, B6, C12 and F8, respectively. The estimated inventories of $^{239+240}Pu$ and mean $^{240}Pu/^{239}Pu$ atom ratios in this and previous study are summarized in Table 1. Combined with the previously reported data (Table 1), the $^{239+240}Pu$ inventory in the ECS varied widely, from 2±0.1 to 807±7 Bq m^{-2}. Higher inventories, with two peak values in the Yangtze Estuary and the south Hangzhou Bay (Fig. 6), have been observed and are apparently higher than those expected from direct atmospheric deposition (36 - 42 Bq m^{-2}) at 20 °N - 40 °N (Kelley et al. 1999); this is likely due to the intense scavenging of particle-reactive radionuclides resulting from higher particle fluxes in these two areas (Che et al., 2003; Huang et al., 2013). Both $^{239+240}Pu$ and $^{210}Pb_{ex}$ inventories in core E1 were lower than the reported values in the same area prior to 1999 (Fig.1, 420 Bq m^{-2} and 21 kBq m^{-2} for $^{239+240}Pu$ and $^{210}Pb_{ex}$, respectively; Su and Huh, 1999). There is steady sediment supply to the Zhe-Min coast carried by ZFCC each year, thus, the inventory reduction in the Zhe-Min coast was not likely caused by sediment erosion; instead, the notable sediment focusing indicated by the ^{234}Th in this region may result in this reduction (Wang et al., 2016) in some areas and increased inventories in other areas, depending on the bottom water currents. However, the reduction of Yangtze sediment discharge has been suggested to lead to the erosion occurring in the Yangtze Estuary during past decade (Yang et al., 2011). In Yangtze Estuary, the erosion is likely one of the important reasons for the reduction in the sedimentary $^{239+240}Pu$ inventory, from 807 Bq m^{-2} obtained in 1997 (BC16, Su and Huh, 2002) to ~400 Bq m^{-2} obtained in 2006 (station 18 and SC07, Liu et al., 2011; Pan et al., 2011).

In order to estimate the PPG Pu contribution to sediment column of the ECS, the mean value of $^{240}Pu/^{239}Pu$ atom ratios in sediment cores were calculated using the equation:

$$R = \frac{\lambda_2 W_1}{\lambda_1 W_2} \quad (3)$$

where W_1 and W_2 are the inventory (Bq m^{-2}) of ^{240}Pu and ^{239}Pu, respectively, and λ_1 and λ_2 are the decay constants of ^{240}Pu (2.89×10^{-7} s^{-1}) and ^{239}Pu (7.88×10^{-8} s^{-1}), respectively. The calculated $^{240}Pu/^{239}Pu$ atom ratios are given in Table 1, together with thedata from published literature. The values range from 0.223 ± 0.022 to 0.300 ± 0.012 (mean: 0.247 ± 0.021). Using these values, the Pu contribution from the PPG input was estimated to be 45%±4% (R_P=0.36) - 52%±4% (R_P=0.33) based on the geometric mean value (0.247±0.021) of $^{240}Pu/^{239}Pu$ atom ratio (Table 1).

3.5 The mass balance of Pu in the ECS sediments

The sources of Pu buried in the ECS potentially include Yangtze River input, global fallout in ECS, PPG input and the Pu derived adjoining the ECS waterbodies. A simple mass balance was used to estimate the contribution of Pu from different sources. The total surface area of ECS corresponding to the $^{239+240}$Pu inventories was estimated by Google Earth to be 3.28×10^{11} m^2. The inventory of $^{239+240}$Pu from global fallout was reported to be 36 Bq m^{-2} between 20 °N and 30 °N and 42 Bq m^{-2} between 30 °N and 40 °N (UNSCEAR, 2000); here we used the mean value (39±4 Bq m^{-2}) and estimated the total global Pu (direct atmospheric deposition) in the ECS to be (1.3±0.1) $\times 10^{13}$ Bq. Using the arithmetic mean value of the $^{239+240}$Pu inventory in four segments of the ECS (details are shown in supplementary materials), the total buried Pu was estimated to be (3.1 ± 1.4) $\times 10^{13}$ Bq. The PPG input was estimated to be (1.4 ± 0.7) $\times 10^{13}$ - (1.6 ± 0.7) $\times 10^{13}$Bq by total Pu × Pu fraction of Pu derived from PPG. Moreover, the total inventory of the Yangtze input of $^{239+240}$Pu during 61 years (1952-2013) was estimated to be (0.15 ± 0.08) × 10^{13} Bq based on the annual input rate from Yangtze River of (2.4 ± 1.4) × 10^{10} Bq. Besides, we can observe that there was other source of Pu to the ECS with value of (0.06±0.05) × 10^{13} – (0.28±0.24) × 10^{13} Bq, characterized by the global fallout ^{240}Pu/^{239}Pu atom ratio. Previous studies (Liu et al., 2003) had suggested that the finer part of sedimentary material of the Yellow River could be transported southward into the ECS, especially influenced by the strong southward coastal current during winter. Dai et al. (2011) reported that a small portion of sediment in the North Jiangsu coast could be transported into the north branch of the Yangtze River driven by the NJCC and then entered the ECS. Meanwhile, the ^{240}Pu/^{239}Pu atom ratios in Lanzhou (the Yellow River catchment) and the North Jiangsu tidal flats were also reported to be ~ 0.18 (Zheng et al., 2009; Liu et al., 2013). Considering all the observations above, we suggest that there is a small fraction of Pu that originated from the Yellow River and North Jiangsu coast that could be transported from the Yellow Sea to the ECS by the coastal currents. It is also anticipated that the contribution of the Yellow sea to the ECS will likely vary spatially within the ECS. Finally, we attempted to construct a mass balance (Fig. 7) of sedimentary $^{239+240}$Pu for sediment in the ECS. Although the Yangtze River input is the important Pu source for the estuary area of the Yangtze River, it is relatively small compared to the entire inventory of Pu in the ECS, and the dominant contribution of $^{239+240}$Pu to the ECS remains from the PPG by the KC.

The TWC and the KC bring many nutrients to the ECS, with very volume of water of 7.9×10^{14} m^3 y^{-1} and 4.1×10^{13} m^3 y^{-1}, respectively (Kagimoto and Yamagata,

1997; Su, 2001). The mean $^{239+240}$Pu activity in the upper 200 m of sea water in the northeast of the Taiwan Island and near the KC was reported to be 3.3±2.7 mBq m^{-3} (CB-11; 25.24 °N, 124.52 °E; Nagaya and Nakamura, 1992), a value that is comparable to the decades mean value of surface water in the western Pacific Ocean (2.4 - 3.6 mBq m^{-3}, Povinec et al., 2005). Using the mean $^{239+240}$Pu activity (3.3 mBq m^{-3}) and multiplying the total flow of the KC and TWC for 61 years (1952-2013), we can roughly estimate that (1.6±1.3) × 10^{14} Bq $^{239+240}$Pu passed through the ECS by the KC and TWC during the past six decades. Therefore, the buried $^{239+240}$Pu in sediments of ECS accounted for 8.8% ± 8.3% - 10.0% ± 9.2% of the total $^{239+240}$Pu transported by the KC and TWC into the ECS. It should be noted that $^{239+240}$Pu concentration in the KC seawater might be much higher in 1950's than present; and these reported values in the seawater column might not include the particle associated Pu, so the estimation here might be a higher estimate. Considering the very high Pu contribution from the PPG input, the ^{240}Pu/^{239}Pu atom ratio can not only be potentially used to obtain a better insight of the biogeochemistry influenced by the KC, but also used to trace the long-range transport of other particle-reactive radionuclides such as ^{210}Pb, ^{230}Th, ^{231}Pa, and other particle-reactive species.

5. Conclusion

Based on the Pu isotopic analysisand $^{210}Pb_{ex}$ in the sediments of the ECS, the following conclusions are drawn:

The $^{239,\ 240}$Pu activity concentrations in the ECS surface sediments ranged between 0.048 and 0.492 Bq kg^{-1} (mean: 0.188 ± 0.007 Bq kg^{-1}). The ^{240}Pu/^{239}Pu atom ratios in the ECS, ranging from 0.158 to 0.297 (mean: 0.234 ± 0.024), exhibited a distribution pattern similar to that of the $^{239,\ 240}$Pu activities. The atom ratios were mostly higher than the global fallout value of 0.18 and were lower than the signature value (0.36) of the PPG, which indicates an influence of PPG Pu input to the ECS. The sedimentation rates estimated from the penetration depths of $^{239+240}$Pu were similar to the values based on $^{210}Pb_{ex}$ at cores E1, M7, B6, C12 and F8. Compared to ^{137}Cs, $^{239+240}$Pu is a better time marker and can be used to calibrate the $^{210}Pb_{ex}$ chronology in marine environment.

The annual Yangtze River input of $^{239+240}$Pu is estimated to be 2.4 ×10^{10} Bq, which is small compared to the total Pu inventory of 3.1×10^{13} Bq in the ECS shelf. However, the estimated $^{239+240}$Pu concentration in the suspended material in the Yangtze River (0.18 Bq kg^{-1}) is within the range of the values found in the Yangtze Estuary sediments, and the ^{240}Pu/^{239}Pu atom ratios are ~ 0.18, which indicates that the

Yangtze River input dominates as the source of Pu in the estuary area in the ECS. The estimated PPG input of $^{239+240}$Pu is (1.4-1.6)×10^{13} Bq, which accounts for 45%-52% of the total Pu estimated in the entire ECS and the scavenging ratio of the total $^{239+240}$Pu transported by the KC and TWC into ECS sediments is estimated to be ~10%. These Pu inputs were mainly deposited in coastal and shelf regions via scavenging process. Moreover, a small proportion of Pu could also have been transported from the Yellow Sea to the ECS by the coastal currents. ^{240}Pu/^{239}Pu atom ratio can not only be potentially used to obtain a better insight of the biogeochemistry influenced by the KC, but also be used to trace the long-range transport of other particle-reactive radionuclides such as ^{210}Pb, ^{230}Th, ^{231}Pa, and other particle-reactive organic and inorganic species that have similar K_ds as Pu.

Acknowledgements

This research was supported by the Ministry of Science and Technology of PR China (2011CB409801), the U.S. National Science Foundation (OCE-1237059), the China Scholarship Council (No. 201406140049) and the Fund of ECNU for Overseas Scholars. One of the authors, Mark Baskaran, is thankful for the support from the "*High-end Foreign Experts Recruitment Program*" sponsored by the State Administration of Foreign Affairs (P. R. China). We thank Editor, Dr. Martin Frank and two anonymous reviewers for their constructive comments for improvement of the original manuscript.

References

Baskaran, M., Asbill, S., Santschi, P., Brooks, J., Champ, M., Adkinson, D., Colmer, M. R., Makeyev, V., 1996. Pu, ^{137}Cs and excess ^{210}Pb in Russian Artic sediments. Earth Planet. Sci. Lett. 140, 243–257.

Baskaran, M., Ravichandran M., Bianchi T. S., 1997. Cycling of ^{7}Be and ^{210}Pb in a high DOC, shallow, turbid estuary of southeast Texas. Estuarine Coastal Shelf Sci. 45, 165-176.

Bu, W. T., Zheng, J., Guo, Q. J., Uchida, S., 2014. Vertical distribution and migration of global fallout Pu in forest soils in southwestern China. J. Environ. Radioact. 136, 174–180.

Buesseler, K. O., 1997. The isotopic signature of fallout plutonium in the North Pacific. J. Environ. Radioact. 36, 69.

Buffoni, G., Delfanti, R., Papucci, C., 1992. Accumulation rates and mixing processes in near-surface North Atlantic sediments: Evidence from C-14 and Pu-239,240 downcore profiles. Mar. Geol. 109 (1-2), 159-170.

Che, Y., He, Q., Lin, W. Q., 2003. The distributions of particulate heavy metals and its indication to the transfer of sediments in the Changjiang Estuary and Hangzhou Bay, China. Mar. Pollut. Bull. 46(1), 123-131.

China Water Resources Committee (CWRC), 2013. China River Sediment Bulletin. Ministry of Water Resources of China (ed.) China Water Power Press, Beijing (in Chinese).

Clark, M. J., Smith, F. B., 1988. Wet and dry deposition of Chernobyl releases. Nature 332, 245 – 249.

Cochran, J. K., Hirschberg, D. J., Livingston, H. D., Buesseler, K. O., Key, R. M., 1995. Natural and anthropogenic radionuclide distributions in the Nansen Catchment, Arctic Ocean: Scavenging rates and circulation timescales. Deep Sea Res. Part II, 42, 1495–1517.

Dai, Z. J., Du, J. Z., Chu, A., Zhang, X. L., 2011. Sediment characteristics in the North Branch of the Yangtze Estuary based on radioisotope tracers. Environ. Earth Sci. 62(8), 1629-1634.

Dai, Z. J., Liu, J. T., 2013. Impacts of large dams on downstream fluvial sedimentation: an example of the Three Gorges Dam (TGD) on the Changjiang (Yangtze River). J. Hydrol. 480, 10-18.

Dai, Z., Liu, J., Wei, W., Chen J., 2014. Detection of the Three Gorges Dam influence on the Changjiang (Yangtze River) submerged delta. *Sci. Rep*. 4, 6600, doi:10.1038/srep06600.

DeMaster, D. J., Kuehl, S. A., Nittrouer, C. A., 1986. Effects ofsuspended sediments on geochemical processes near the mouth of the Amazon River: examination of biological silica uptake and the fate of particle-reactive elements. Cont. Shelf Res. 6,107– 125.

Delfanti, R., Klein, B., Papucci, C., 2003. Distribution of ^{137}Cs and other radioactive tracers in the eastern Mediterranean: Relationship to the deepwater transient. J. Geophys. Res. 108(C9), 8108, doi:10.1029/2002JC001371.

Dominik, J., Burrus, D. Vernet, J. P., 1987. Transport of the environmental radionuclides in an alpine watershed. Earth Planet. Sci. Lett. 84, 165–180.

Donaldson L. R., Seymour A. H., Nevissi A. E., 1997. University of Washington's radioecological studies in the Marshall Islands, 1946–1997. Health Physics 73, 214 – 222.

Dong, W., Tims, S. G., Fifield, L. K., Guo, Q. J., 2010. Concentration and characterization of plutonium in soils of Hubei in central China. J. Environ. Radioact. 101, 29–32.

Dou, Y., Yang, S., Liu, Z., Clift, P. D., Shi, X., Yu, H. Berne, S., 2010. Provenance discrimination of siliciclastic sediments in the middle Okinawa Trough since 30 ka: Constraints from rare earth element compositions. Mar. Geol. 275(1), 212-220.

Du, J., Wu, Y., Huang, D., Zhang, J., 2010, Use of ^{7}Be, ^{210}Pb and ^{137}Cs tracers to the transport of surface sediments of the Changjiang Estuary, China, J. Mar. Syst. 82 (4), 286–294.

Hamilton, T. F., 2004. Linking legacies of the cold war to arrival of anthropogenic radionuclides in the oceans through the 20th century. Marine radioactivity 6, 30-87.

Hu, D., Wu, L., Cai, W., Gupta, A. S., Ganachaud, A., Qiu, B., Gordon, A. L., Lin, X., Chen, Z., Hu, S., Wang, G.,Wang, Q., Sprintall, J., Qu, T., Kashino, Y., Wang, F.,

Kessler, W., 2015. Pacific western boundary currents and their roles in climate. Nature 522(7556), 299-308.

Huang, D., Du, J., Moore, W. S., Zhang, J. 2013. Particle dynamics of the Changjiang Estuary and adjacent coastal region determined by natural particle‐reactive radionuclides (^{7}Be, ^{210}Pb, and ^{234}Th). J. Geophys. Res. Oceans 118(4), 1736-1748.

Huh, C. A., Su, C. C., 1999. Sedimentation dynamics in the East China Sea elucidated from ^{210}Pb,^{137}Cs, and ^{239,240}Pu. Mar. Geol. 160,183–196.

Kagimoto, T., Yamagata, T., 1997. Seasonal transport variations of the Kuroshio: An OGCM simulation. J. Phys. Oceanogr. 27(3), 403-418.

Kelley, J. M., Bond, L. A., Beasley, T. M., 1999. Global distribution of Pu isotopes and ^{237}Np. Sci. Total Environ. 237/238, 483–500.

Kersting, A. B., Efurd, D. W., Finnegan, D. L., Rokop, D. J., Smith, D. K., Thompson, J. L., 1999. Migration of plutonium in ground water at the Nevada Test Site. Nature 397(6714), 56-59.

Kim C. K., Kim C. S., Chang B. U., Choi S.W., Chung C. S., Hong G. H., Hirose, H., Igarashi, Y., 2004. Plutonium isotopes in seas around the Korean Peninsula. Sci. Total Environ. 318, 197 – 209.

Krey, P. W., Hardy, E. P., Pachucki, C., Rourke, F., Coluzza, J., Benson, W. K., 1976. Mass isotopic composition of global fallout plutonium in soil. Transuranium Nuclides in the Environment (Proceedings Series); IAEA: Vienna, pp 671 −678.

Lee, S. Y., Huh, C. A., Su, C. C., You, C. F., 2004. Sedimentation in the Southern Okinawa Trough: enhanced particle scavenging and teleconnection between the Equatorial Pacific and western Pacific margins. Deep Sea Res. Part I: Oceanographic Research Papers, 51(11), 1769-1780.

Li, Z, Q., Wu, Y., Liu S. M., Du, J. Z., Zhang, J., 2015. An 800-year record of terrestrial organic matter from the East China Sea shelf break: Links to climate change and human activity in the Changjiang Catchment. Deep-Sea Res. II. 113, 1-10.

Liao, H., Zheng, J., Wu, F., Yamada, M., Tan, M., Chen, J., 2008. Determination of plutonium isotopes in freshwater lake sediments by sector-field ICP-MS after separation using ion-exchange chromatography. Appl. Radio. Isot. 66(8), 1138-1145.

Lindahl, P., Asami, R., Iryu, Y., Worsfold, P., Keith-Roach, M., Choi, M. S., 2011. Sources of plutonium to the tropical Northwest Pacific Ocean (1943–1999) identified using a natural coral archive. Geochim. Cosmochim. Acta 75(5), 1346-1356.

Liu, J. P, Li, A. C., Xu, K. H., Velozzi, D. M., Yang, Z. S, Milliman, J. D., DeMaster, D. J., 2006. Sedimentary features of the Changjiang River-derived along-shelf clinoform deposit in the East China Sea. Cont. Shelf Res. 26, 2141-2156.

Liu, J., Zhu, R. X., Li, G. X., 2003. Rock magnetic properties of the fine grained sediment on the outer shelf of the East China Sea: implication for provenance. Mar. Geol. 193,195– 206.

Liu, S., Zhang, W., He, Q., Li, D., Liu, H. Yu, L., 2010. Magnetic properties of East China Sea shelf sediments off the Yangtze Estuary: Influence of provenance and particle size. Geomorphology 119(3), 212-220.

Liu, Z. Y., Zheng J., Pan S., Dong W., Yamada M., Aono, T., Guo Q., 2011. Pu and

^{137}Cs in the Yangtze River Estuary sediments: Distribution and Source Identification. Environ. Sci. Technol. 45 (5), 1805-1811.

Liu, Z. Y., Zheng, J., Pan, S. M., Gao, J. H., 2013. Anthropogenic plutonium in the North Jiangsu tidal flats of the Yellow Sea in China. Environ Monit Assess. 185, 6539–6551.

McKee, B.A., Nittrouer, C.A., DeMaster, D.J., 1983. The concepts of sediment deposition and accumulation applied to the continental shelf near the mouth of the Changjiang River. Geology 11, 631– 633.

Moon, D., Hong, G., Kim, Y.I., Baskaran, M., Chung, C.S., Kim, S.H., 2003. Accumulation of anthropogenic and natural radionuclides in bottom sediments of the Northwest Pacific Ocean. Deep-Sea Res. Part II: Topical Studies in Oceanography 50 (17-21), 2649-2673.

Muramatsu, Y., Uchida S., Tagami K., Yoshida, S., Fujikawa, T., 1999. Determination of plutonium concentration and its isotopic ratio in environmental materials by ICP-MS after separation using and extraction chromatography. J. Anal. Atom. Spectrom. 14(5), 859-865.

Muramatsu, Y., Hamilton, T., Uchida, S., Tagami, K., Yoshida, S., Robison, W., 2001. Measurement of ^{240}Pu/^{239}Pu isotopic ratios in soils from the Marshall Islands using ICP-MS. Sci. Total Environ. 278(1), 151-159.

Nagaya, Y., Nakamura, K., 1992. ^{239,240}Pu and ^{137}Cs in the east China and the Yellow seas. J. Oceanogr. 48, 23–35.

Olsen, C.R., Thein, M., Larsen, I. L., Lowry, P. D., Mulholland, P. J., Cutshall, N. H., Byrd, J. T., Windom, H. L., 1989. Plutonium, lead-210, and carbon isotopes in the Savannah estuary: riverborne versus marine sources. Environ. Sci. Technol. 23, 1475-1481.

Oguri, K., Matsumoto, E., Yamada, M., Saito, Y., Iseki, K., 2003. Sediment accumulation rates and budgets of depositing particles of the East China Sea. Deep Sea Res. Part II: Topical Studies in Oceanography 50(2), 513-528.

Pan, S. M., Tims, S. G., Liu, X. Y., Fifield, L. K., 2011. ^{137}Cs, $^{239+240}$Pu concentrations and the ^{240}Pu/^{239}Pu atom ratio in a sediment core from the sub-aqueous delta of Yangtze River estuary. J. Environ. Radioact. 102(10), 930-936.

Peirson, D. H., Cambray, R. S., Cawse, P. A., Eakins, J. D., Pattenden, N. J., 1982. Environmental radioactivity in Cumbria. Nature 300, 27-32.

Povinec, P.P., Livingston, H.D., Shima, S., Aoyama, M., Gastaud, J., Goroncy, I., Hirose, K., Huynh-Ngoc, L., Ikeuchi, Y., Ito, T., La Rosa, J., Kwong, L.L.W., Lee, S.H., Moriya, H., Mulsow, S., Oregioni, B., Pettersson, H., Togawa, O., 2003. IAEA'97 expedition to the NW Pacific Ocean-results of oceanographic and radionuclide investigations of the water column. Deep-Sea Res. II 50, 2607–2637.

Povinec, P. P., Aarkrog, A., Buesseler, K. O., Delfanti, R., Hirose, K., Hong, G. H., Ito, T., Livingston, H. D., Niles, H., Noshkin, V. E., Shima, S., Togawa, O., 2005. ^{90}Sr, ^{137}Cs and ^{239,240}Pu concentration surface water time series in the Pacific and Indian Oceans–WOMARS results. J. Environ. Radioact. 81(1), 63-87.

Qiao, J., Shi, K., Hou, X., Nielsen, S., Roos, P., 2014. Rapid multisample analysis for simultaneous determination of anthropogenic radionuclides in marine environment. Environ. Sci. Technol. 48(7), 3935-3942.

Ravichandran, M., Baskaran, M., Santschi, P. H., Bianchi, T. S., 1995. Geochronology of sediments in the Sabine-Neches estuary, Texas, USA. Chem.

696 Geol. 125, 291-306.
697 Santschi, P. H., Li. Y. H., Bell, J. J., Trier, R. M., Kawtaluk, K., 1980. Pu in coastal
698 marine environment. Earth Planet. Sci. Lett. 51, 248-265.
699 Scott, M. R., Rotter, R. J., Salter, P. F., 1985. Transport of fallout plutonium to the
700 ocean by the Mississippi River. Earth Planet. Sci. Lett. 75(4), 321-326.
701 Smith, J. N., Ellis, K. M., Nelson, D. M., 1987. Time-dependent modeling of fallout
702 radionuclide transport in a drainage catchment: significance "of slow" erosional and
703 fast hydrological components. Chem. Geol. 63, 157–180.
704 Su, C. C., Huh, C. A., 2002. ^{210}Pb, ^{137}Cs and $^{239;240}$Pu in East China Sea sediments:
705 sources, pathways and budgets of sediments and radionuclides. Mar. Geol. 183,
706 163-178.
707 Su, J. L. 2001. A review of circulation dynamics of the coastal oceans near China (in
708 Chinese with English abstract). Acta Oceanol. Sin. 23(4), 1–16.
709 UNSCEAR, United Nations Scientific Committee on the Effects of Atomic Radiation
710 Exposures to the Public from Man-made Sources of Radiation, Sources and Effects
711 of Ionizing Radiation, United Nations, New York, 2000, 654 pp.
712 Wang, J., Du, J., Baskaran, M., Zhang, J., 2016. Mobile mud dynamics in the East
713 China Sea elucidated using ^{210}Pb, ^{137}Cs, ^{7}Be, and ^{234}Th as tracers, J. Geophys. Res.
714 Oceans 121, 224-239.
715 Wang, Z. L., Yamada, M., 2005. Plutonium activities and ^{240}Pu/^{239}Pu atom ratios in
716 sediment cores from the East China Sea and Okinawa Trough: Sources and
717 inventories. Earth Planet. Sci. Lett. 233, 441–453.
718 Wu, F., Zheng, J., Liao, H., Yamada, M., 2010. Vertical distributions of plutonium and
719 ^{137}Cs in lacustrine sediments in northwestern China: quantifying sediment
720 accumulation rates and source identifications. Environ. Sci. Technol. 44(8),
721 2911-2917.
722 Wu, H., 2015. Cross-shelf penetrating fronts: A response of buoyant coastal water to
723 ambient pycnocline undulation. J. Geophys. Res. Oceans 120(7), 5101-5119.
724 Wu, J., Zheng, J., Dai, M., Huh, C. A., Chen, W., Tagami, K., Uchida, C., 2014.
725 Isotopic Composition and Distribution of Plutonium in Northern South China Sea
726 Sediments Revealed Continuous Release and Transport of Pu from the Marshall
727 Islands. Environ. Sci. Technol. 48, 3136 −3144.
728 Xu, Y., Qiao, J., Hou, X., Pan, S., Roos, P., 2014. Determination of plutonium
729 isotopes (^{238}Pu, ^{239}Pu, ^{240}Pu, ^{241}Pu) in environmental samples using radiochemical
730 separation combined with radiometric and mass spectrometric measurements.
731 Talanta 119, 590–595.
732 Yamada, M., Zheng, J., Wang, Z. L., 2006. ^{137}Cs, $^{239+}$ ^{240}Pu and ^{240}Pu/^{239}Pu atom
733 ratios in the surface waters of the western North Pacific Ocean, eastern Indian
734 Ocean and their adjacent seas. Sci. Total Environ. 366(1), 242-252.
735 Yang, S. L., Milliman, J. D., Li, P., Xu, K., 2011. 50,000 dams later: erosion of the Yangtze
736 River and its delta. Global Planet. Change 75(1),14-20.
737 Zhao, C., Qiao, F. L., Wang, G. S., Xia, C. S., Jung, K. T., 2014. Simulation and
738 prediction of ^{137}Cs from the Fukushima accident in the China Seas. Science China.
739 (34), 3416-3423.
740 Zheng, J., Yamada, M., 2004. Sediment core record of global fallout and Bikini
741 closein fallout Pu in Sagami Bay, Western Northwest Pacific Margin. Environ. Sci.

Technol. 38, 3498-3504.

Zheng, J., Yamada, M. 2006. Plutonium isotopes in settling particles: transport and scavenging of Pu in the western Northwest Pacific. Environ. Sci. Technol. 40(13), 4103-4108.

Zheng, J., Yamada, M., Wu, F. C., Liao, H. Q., 2009. Characterization of Pu concentration and its isotopic composition in soils of Gansu in the northwestern China. J. Environ. Radioact. 100, 71–75.

Zheng, J., Aono, T., Uchida, S., Zhang, J., Honda, M. C., 2012. Distribution of Pu isotopes in marine sediments in the Pacific 30 km off Fukushima after the Fukushima Daiichi nuclear power plant accident. Geochem. J., 46(4), 361-369.

Figure Captions

Figure 1 Location of sites occupied during the August cruise tracts in 2013 (surface sediment in blue and sediment core in purple). Several sediment cores from literature are marked in red color (6, BC16, Su and Huh, 2002; 18, Liu et al., 2011; SC07, Pan et al., 2011). Bathymetry (m) of the ECS shelf is also shown by grey lines. The summer regional surface currents are modified after Su, 2001 and Hu et al., 2015: Changjiang diluted water (CDW, Summer); Zhejiang-Fujian Coast Current (ZFCC, Winter); North Jiangsu Coast Current (NJCC); Yellow Sea Coastal Current (YSCC); Yellow Sea Warm Current (YSWC); Taiwan Warm Current (TWC); Kuroshio Current (KC); North Equatorial Current (NEC); Mindanao Current (MC). Several rivers are also plotted, including a: Yellow River (5460 km), b: Yangtze River (6400 km), c: Qiantang River (589 km), d: Jiao River (206 km), e: Ou River (384 km), f: Min River (562 km).

Figure 2 Spatial distribution of the ^{239}Pu, ^{240}Pu, $^{239+240}Pu$ activities and $^{240}Pu/^{239}Pu$ atom ratios of surface sediment in August of 2013.

Figure 3 The synthesis of $^{240}Pu/^{239}Pu$ atom ratios in the areas surrounding the ECS: Chinese and Japanese soil (black color, Muramatsu et al., 1999, 2003; Zheng et al., 2009; Dong et al., 2010; Liu et al., 2013； Bu et al., 2014), sediment (red color, This study; Buesseler, 1997; Zheng and Yamada, 2004; Wang and Yamada, 2005; Liu et al., 2011; Wu et al., 2014), seawater (blue color, Kim et al., 2004; Yamada et al., 2006) and a natural coral (orange color, Lindahl et al., 2011).

Figure 4 Distribution of $\ln(^{210}Pb_{ex})$ and ^{137}Cs activities in sediment cores collected from the ECS at six stations: estuary (C1), South inshore (E1), North offshore (M7, B7), and Okinawa trough (C12, F8).

Figure 5 $^{239+240}Pu$, and $^{240}Pu/^{239}Pu$ atom ratios in sediment cores collected from the ECS at six stations.

Figure 6 Spatial distribution of $^{239+240}Pu$ inventories in sediment, including literature datas (Nagaya and Nakamura, 1992; Su and Huh, 1999; 2002; Wang and Yamada, 2005; Pan et al., 2011; Liu et al., 2011).

Figure 7 The mass balance of $^{239+240}Pu$ in sediment in the ECS.

Fig 1

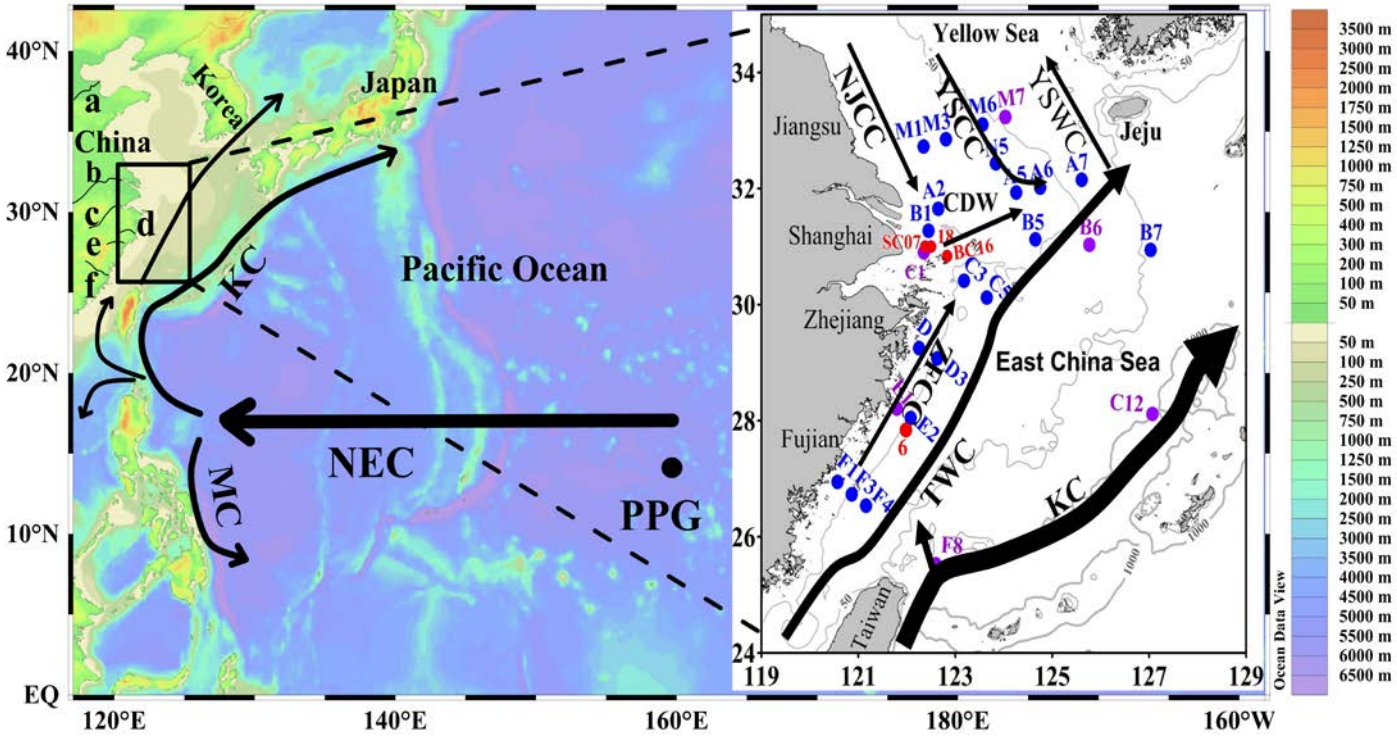
40°N
30°N
20°N
10°N
EQ
120°E
140°E
160°E
180°E
160°W
a
China
b
c
d
e
f
Korea
Japan
Pacific Ocean
KC
NEC
MC
PPG
Yellow Sea
Jiangsu
Shanghai
Zhejiang
Fujian
Taiwan
Jeju
East China Sea
NJCC
YSCC
YSWC
CDW
TWC
KC
34
32
30
28
26
24
119
121
123
125
127
129
Ocean Data View
3500 m
3000 m
2500 m
2000 m
1750 m
1500 m
1250 m
1000 m
750 m
500 m
400 m
300 m
200 m
100 m
50 m
50 m
100 m
250 m
500 m
750 m
1000 m
1250 m
1500 m
2000 m
2500 m
3000 m
3500 m
4000 m
4500 m
5000 m
5500 m
6000 m
6500 m

Fig 2

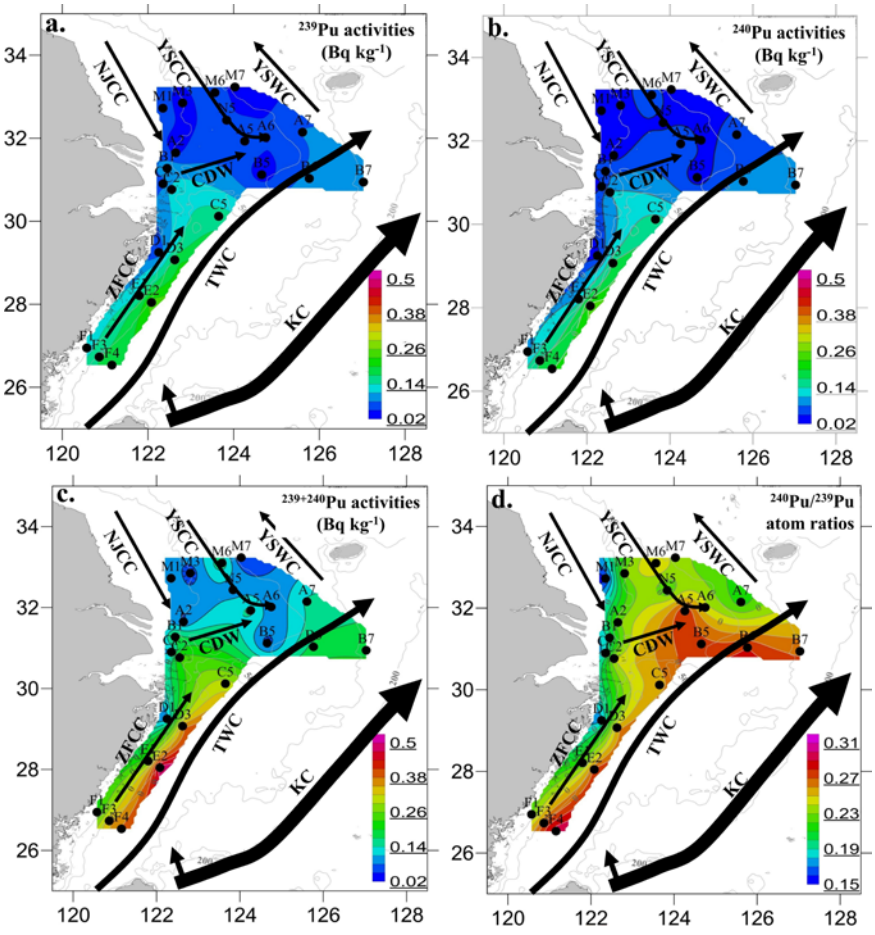
a.
239Pu activities (Bq kg-1)
b.
240Pu activities (Bq kg-1)
c.
239+240Pu activities (Bq kg-1)
d.
240Pu/239Pu atom ratios
NJCC
YSCC
YSWC
CDW
ZFCC
TWC
KC
0.5
0.38
0.26
0.14
0.02
0.31
0.27
0.23
0.19
0.15
120
122
124
126
128
26
28
30
32
34

Fig 3

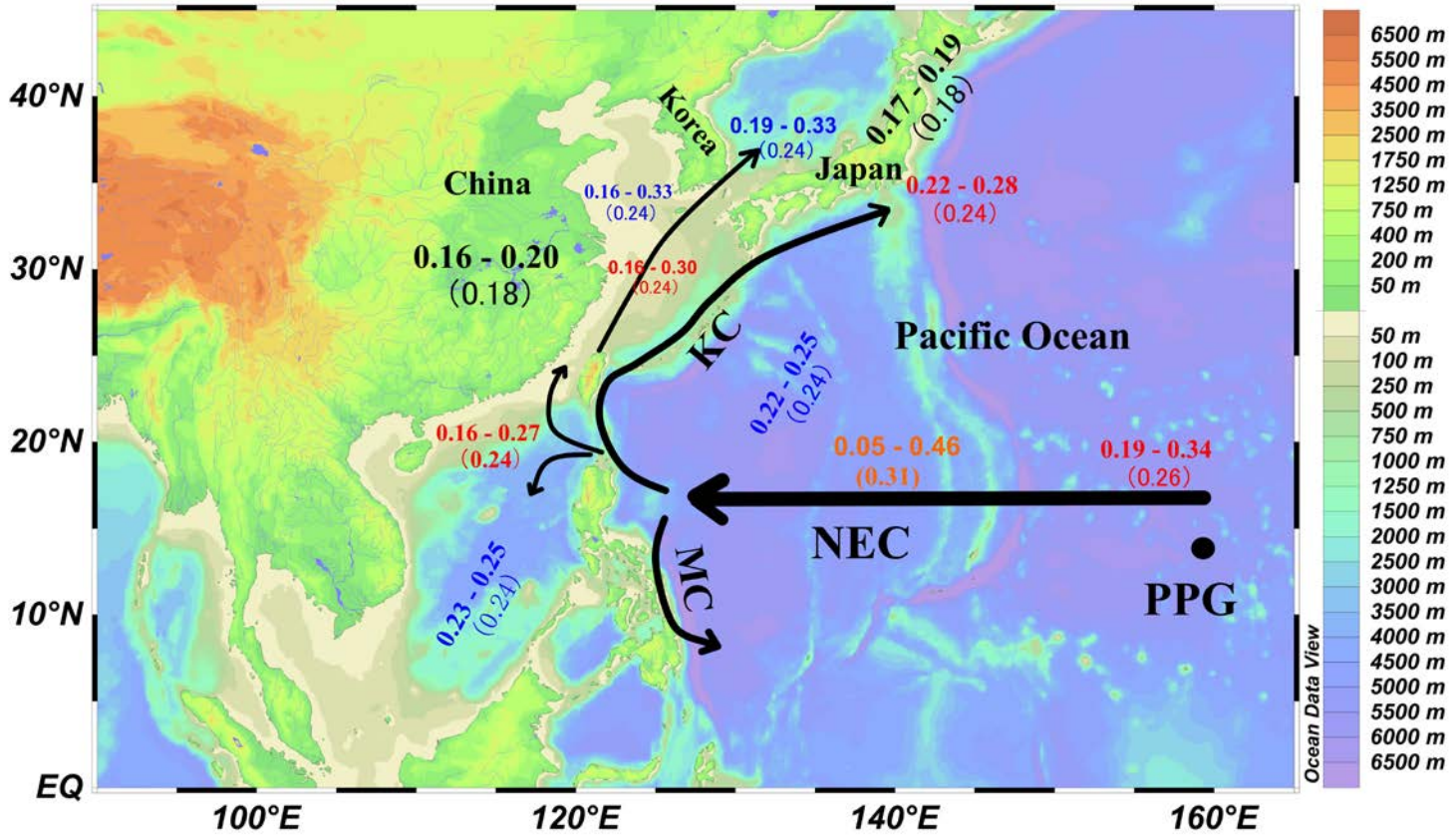
40°N
30°N
20°N
10°N
EQ
100°E
120°E
140°E
160°E
China
Korea
Japan
Pacific Ocean
0.16 - 0.20
(0.18)
0.19 - 0.33
(0.24)
0.17 - 0.19
(0.18)
0.16 - 0.33
(0.24)
0.22 - 0.28
(0.24)
0.16 - 0.30
(0.24)
KC
0.22 - 0.25
(0.24)
0.16 - 0.27
(0.24)
0.05 - 0.46
(0.31)
0.19 - 0.34
(0.26)
NEC
MC
PPG
0.23 - 0.25
(0.24)
6500 m
5500 m
4500 m
3500 m
2500 m
1750 m
1250 m
750 m
400 m
200 m
50 m
50 m
100 m
250 m
500 m
750 m
1000 m
1250 m
1500 m
2000 m
2500 m
3000 m
3500 m
4000 m
4500 m
5000 m
5500 m
6000 m
6500 m
Ocean Data View

Fig 4

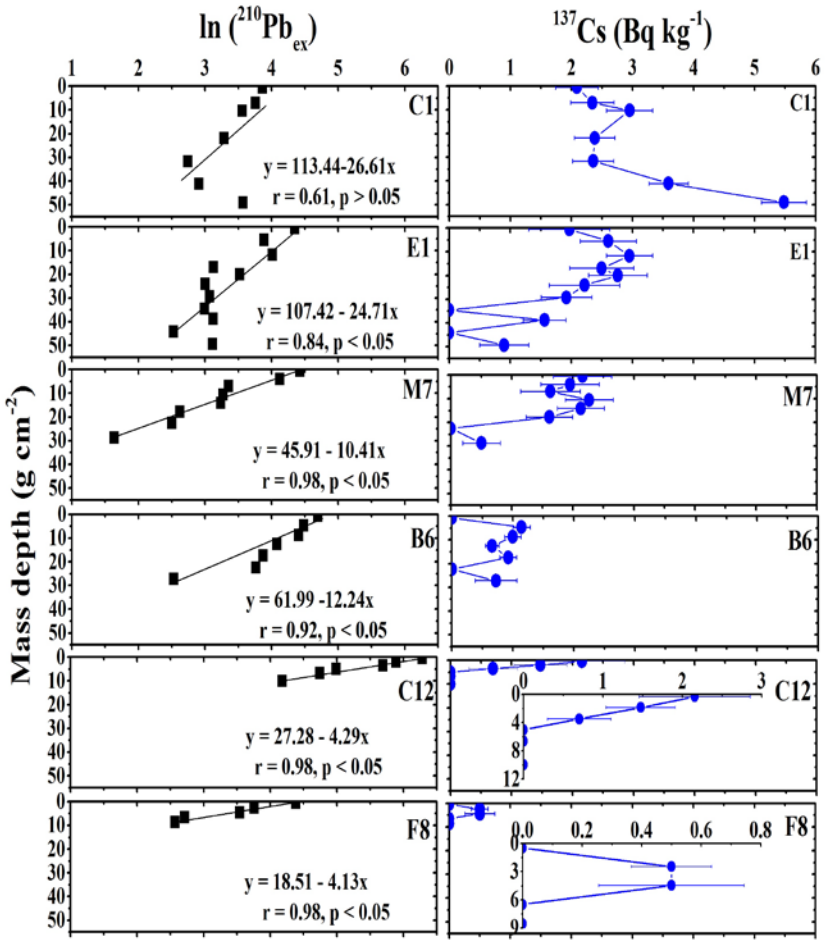
ln (^{210}Pb$_{ex}$)
^{137}Cs (Bq kg^{-1})
Mass depth (g cm^{-2})
C1
y = 113.44-26.61x
r = 0.61, p > 0.05
E1
y = 107.42 - 24.71x
r = 0.84, p < 0.05
M7
y = 45.91 - 10.41x
r = 0.98, p < 0.05
B6
y = 61.99 -12.24x
r = 0.92, p < 0.05
C12
y = 27.28 - 4.29x
r = 0.98, p < 0.05
F8
y = 18.51 - 4.13x
r = 0.98, p < 0.05

Fig 5

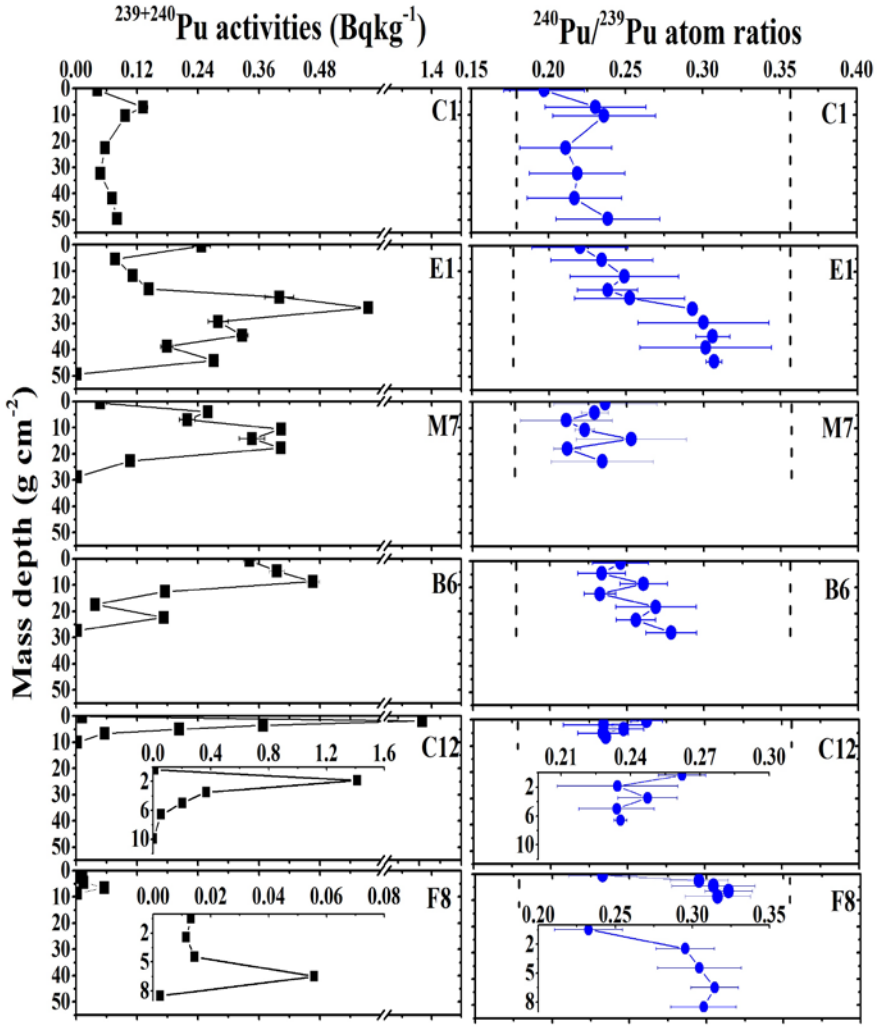
239+240Pu activities (Bqkg-1)
240Pu/239Pu atom ratios
Mass depth (g cm-2)
C1
E1
M7
B6
C12
F8

Fig 6

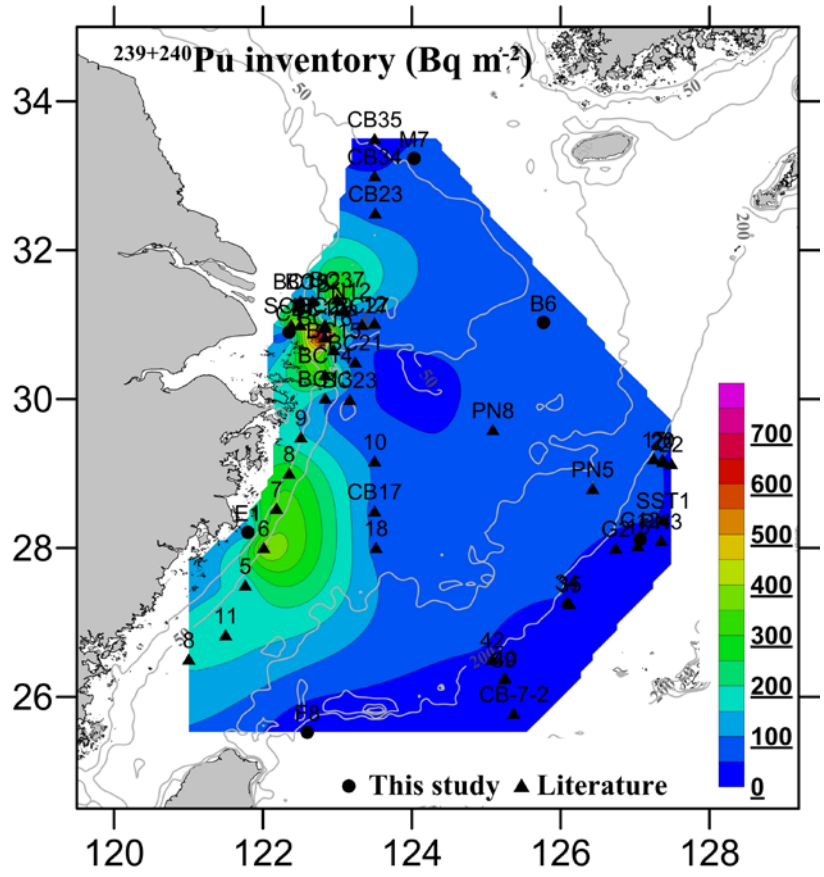
239+240Pu inventory (Bq m-2)
CB35
M7
CB34
CB23
B6
PN8
PN5
CB17
SST1
CB-7-2
700
600
500
400
300
200
100
0
This study
Literature
34
32
30
28
26
120
122
124
126
128

Fig 7

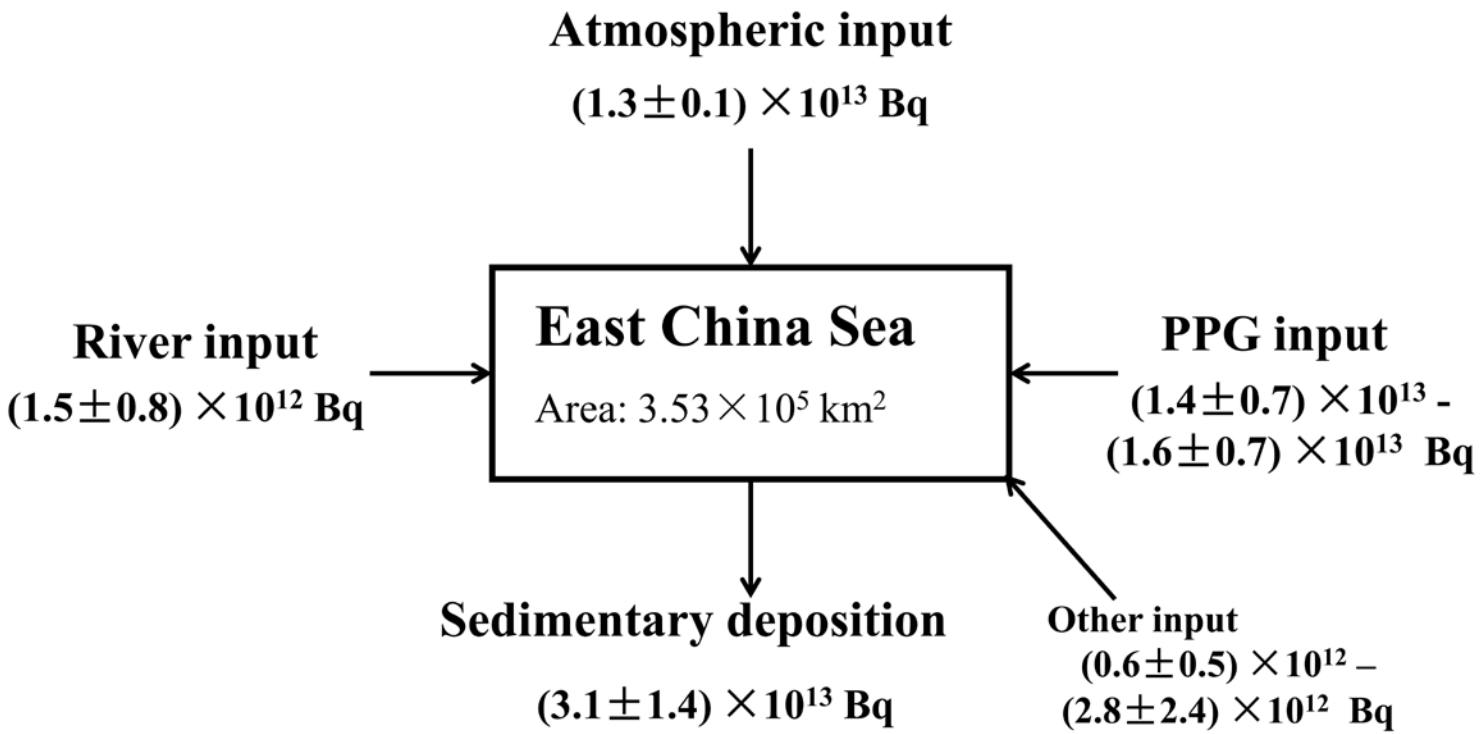
Atmospheric input
(1.3±0.1) ×10^13 Bq
River input
(1.5±0.8) ×10^12 Bq
East China Sea
Area: 3.53×10^5 km^2
PPG input
(1.4±0.7) ×10^13 -
(1.6±0.7) ×10^13 Bq
Sedimentary deposition
(3.1±1.4) ×10^13 Bq
Other input
(0.6±0.5) ×10^12 –
(2.8±2.4) ×10^12 Bq

Table 1
Inventories of ^{239}Pu, ^{240}Pu, $^{239+240}Pu$ and the mean $^{240}Pu/^{239}Pu$ atom ratios in sediment cores from the ECS.

Sample	Longitude (E)	Latitude (N)	Water depth (m)	$^{239+240}Pu$ (Bq m^{-2})	$^{240}Pu/^{239}Pu$	^{239}Pu (Bq m^{-2})	^{240}Pu (Bq m^{-2})	References
Estuary	122-124	30-32	23-58 (42)	48.5-807 (245)				
Inner shelf	120-124	26-30	26-84 (55)	81.7-420 (221)				Su and Huh, 2002
Outer shelf	122.124.5	26-32	55-67 (61)	50.1-117 (83.3)				
Slope	124.5-125	28.5-29.5	232-1053 (735)	16.7-93.3 (43.7)				
CB-7-2	125.37	25.78	2170	8.9 ± 0.3				
CB17	123.50	28.50	65	79.9 ± 2.2				Nagaya and Nakamura, 1992
CB23	123.51	32.50	42	77.4 ± 1.4	No data reported			
CB34	123.50	33.00	37	53.8 ± 1.3				
CB35	123.50	33.50	64	16.2 ± 0.3				
G2	126.74	28.00	999	32.5 ± 2.3	0.245** ± 0.017	17.1 ± 1.2	15.4 ± 1.1	
PN3*	127.35	28.10	1000	47.2 ± 3.1	0.258** ± 0.018	24.2 ± 2.3	23.0 ± 1.1	
SST1*	127.38	28.38	1080	47.0 ± 2.3	0.230** ± 0.012	25.5 ± 1.2	21.5 ± 1.2	Wang and Yamada, 2005
PN5*	126.43	28.80	127	101 ± 5.2	0.263** ± 0.014	51.2 ± 3.2	49.5 ± 2.1	
PN8*	125.09	29.59	87	60.9 ± 4.4	0.254** ± 0.016	31.5 ± 2.3	29.4 ± 1.6	
PN12*	123.08	31.20	50	81.5 ± 3.6	0.242** ± 0.010	43.2 ± 2.1	38.3 ± 1.5	
C1	122.35	30.90	13	35.6 ± 2.5	0.221 ± 0.014	19.6 ± 2.0	16.0 ± 1.6	
E1	121.80	28.21	22	118 ± 5.0	0.270 ± 0.034	58.3 ± 3.3	59.6 ± 3.7	
M7	124.03	33.23	66	65.4 ± 2.5	0.228 ± 0.015	35.8 ± 1.7	29.5 ± 1.8	This study
B6	125.77	31.03	62	58.3 ± 4.6	0.254 ± 0.018	30.7 ± 2.6	27.7 ± 3.7	
C12	127.07	28.12	998	33.9 ± 0.7	0.243 ± 0.012	18.2 ± 0.4	15.7 ± 0.6	
F8	122.60	25.53	619	1.9 ± 0.1	0.291 ± 0.033	0.9 ± 0.0	1.0 ± 0.0	
SC07*	122.38	31.00	14	407 ± 27.0	0.242** ± 0.023	215.7 ± 24.9	191.3 ± 30.9	Pan et al., 2011
18*	122.50	31.00	20	388 ± 21.0	0.237** ± 0.011	207.6 ± 20.2	180.4 ± 17.9	Liu et al., 2011

Kommenterede [XH1]: The uncertainty cannot be 0.0. For example, it can be presented as 0.92±0.04, and 1.04±0.04

*: The Pu inventories ($^{239+240}$Pu) were calculated as follows: total inventory of $^{239+240}$Pu in each layer = (mass depth in that layer × (^{239}Pu activity + ^{240}Pu activity in that layer); total $^{239+240}$Pu inventory = summation of inventory in each layer; for all other samples, the total Pu were measured by alpha spectrometry which is a measure of the combined activity of ^{239}Pu and ^{240}Pu, as alpha spectrometry method yields ^{239,240}Pu activity due to overlapping alpha energies of ^{239}Pu and ^{240}Pu.

**: The mean ^{240}Pu/^{239}Pu atom ratios were calculated as follows: the total inventory of $^{239+240}$Pu × the ^{240}Pu/^{239}Pu ratio in each layer / the sum of $^{239+240}$Pu inventory in each layer.

Table 2
Inventories of ^{239}Pu, ^{240}Pu, $^{239+240}Pu$ and the mean $^{240}Pu/^{239}Pu$ atom ratios in sediment cores from the Yangtze River catchment.

Sample	Longitude (E)	Latitude (N)	$^{239+240}Pu$ (Bq m^{-2})	$^{240}Pu/^{239}Pu$	^{239}Pu (Bq m^{-2})	^{240}Pu (Bq m^{-2})	References
Southwest China							
GY*	106.67	26.66	63.0 ± 2.4	0.191** ± 0.010	37.0 ± 2.3	26.0 ± 2.3	
WL*	107.85	29.52	114.0 ± 5.9	0.185** ± 0.004	67.9 ± 5.8	46.1 ± 3.4	Bu et al., 2014
ZX*	107.85	30.53	19.0 ± 1.6	0.182** ± 0.008	11.4 ± 1.6	7.6 ± 1.0	
Central China							
DK*	112.19	31.15	44.9 ± 5.9	0.183** ± 0.052	26.9 ± 5.0	18.0 ± 7.5	Dong et al., 2010
GLZ*	111.42	32.24	54.6 ± 4.4	0.200** ± 0.013	31.5 ± 4.2	23.1 ± 3.4	
Atmospheric fall		20-30	36.0	0.180	21.7	14.3	Kelley et al. 1999; UNSCEAR, 2000
		30-40	42.0		25.3	16.7	

See the footnote in Table 1